The Journal of Experimental Biology 213, 1406-1416

doi:10.1242/jeb.036921

The mechanics of azimuth control in jumping by froghopper insects

G. P. Sutton* and M. Burrows

Department of Zoology, University of Cambridge, Downing Street, Cambridge CB2 3EJ, UK

*Author for correspondence (rscealai@gmail.com)

Accepted 4 January 2010

SUMMARY

Many animals move so fast that there is no time for sensory feedback to correct possible errors. The biomechanics of the limbs participating in such movements appear to be configured to simplify neural control. To test this general principle, we analysed how froghopper insects control the azimuth direction of their rapid jumps, using high speed video of the natural movements and modelling to understand the mechanics of the hind legs. We show that froghoppers control azimuth by altering the initial orientation of the hind tibiae; their mean angle relative to the midline closely predicts the take-off azimuth. This applies to jumps powered by both hind legs, or by one hind leg. Modelling suggests that moving the two hind legs at different times relative to each other could also control azimuth, but measurements of natural jumping showed that the movements of the hind legs were synchronised to within 32 μs of each other. The maximum timing difference observed (67 μs) would only allow control of azimuth over 0.4 deg. to either side of the midline. Increasing the timing differences between the hind legs is also energetically inefficient because it decreases the energy available and causes losses of energy to body spin; froghoppers with just one hind leg spin six times faster than intact ones. Take-off velocities also fall. The mechanism of azimuth control results from the mechanics of the hind legs and the resulting force vectors of their tibiae. This enables froghoppers to have a simple transform between initial body position and motion trajectory, therefore potentially simplifying neural control.

Key words: trajectory control, biomechanics, Hemiptera, Auchenorrhyncha.

INTRODUCTION

Jumping is a ubiquitous behaviour used by many animals for escape, predation, rapid locomotion and, in insects, take-off into flight. Some jumps may simply be the fastest way to escape from hostile surroundings when the overriding demand is to move as rapidly as possible away from a threatening stimulus. On other occasions jumps may need to be directed toward a particular target in the environment as when, for example, a grasshopper jumps from one grass stem to another. Then the accuracy of the movement will depend on the precise control of three variables; the velocity of the movement and its direction in both the azimuth and elevation planes. An inaccurate jump might cause a collision with a plant leaf or stem that would prevent the establishment of flight, or, at worst, cause the insect to ricochet at high speed toward a hungry predator. Furthermore, jumping movements in most insects are so fast, taking less than 1 ms in froghopper insects (Burrows, 2003; Burrows, 2006a) to a few tens of milliseconds in grasshoppers (Bennet-Clark, 1975; Brown, 1967), that there is no time for sensory feedback to make any adjustments. The challenge of jumping is therefore to produce a movement that is both fast and when necessary accurate, without the assistance of sensory feedback.

In locusts, jumping is constrained by the orientation of the hind legs on either side of the body which move in separate planes to each other, and by the structure of the joints and muscles. A jump is powered by muscles in the enlarged hind femora that move the femoro-tibial joints which have their own specialised mechanics for increasing the lever ratios of the flexor and extensor muscles depending on joint position, and for locking the tibiae when they are fully flexed (Heitler, 1974). When jumping to a target, a locust first peers by moving its head from side to side to determine the desired trajectory (Eriksson, 1980; Sobel, 1990). The azimuth direction of the jump is then set by adjusting the orientation of the body to the target by movements of the forelegs (Santer et al., 2005). Elevation is set by rotating the coxae of the hind legs so that the force generated by the extension of the hind tibiae is exerted along a line connecting the distal end of the tibia with the proximal end of the femur (Sutton and Burrows, 2008). The velocity is determined by the force exerted by the femoral muscles that move the hind tibiae, which are controlled by a motor pattern of three phases (Burrows, 1995; Heitler and Burrows, 1977). Normally the two hind legs extend at the same time or within a few milliseconds of each other. The mechanical arrangement of the hind legs means, however, that directed jumps can still be produced even if one leg extends some time before the other, or if only one hind leg is used (Bennet-Clark, 1975; Santer et al., 2005; Sutton and Burrows, 2008). This control strategy may be used by other insects with the same arrangement of their hind legs, such as stick insects (Burrows, 2008), bush crickets [Orthoptera, Tettigoniidae (Burrows and Morris, 2003)], and flea beetles [Coleoptera, Alticinae (Brackenbury and Wang, 1995)].

By contrast, the fastest of the jumping insects, froghoppers (Hemiptera, Auchenorrhyncha, Cercopidae), have their power-producing hind legs slung underneath their body so that both move in the same plane (Burrows, 2003; Burrows, 2006a; Burrows, 2006b). In further contrast, the movements of the hind legs are powered by huge muscles in the thorax that depress the trochantera. These different mechanisms nevertheless allow jumps to be directed toward a target in both elevation and azimuth planes (Brackenbury, 1996). Elevation is now controlled by the front and middle legs that set the attitude of the body relative to the ground before take-off (Burrows, 2006a). Velocity is controlled by a three-phase motor pattern (Burrows, 2007c) that delivers power in a catapult mechanism through the hind legs.

An unresolved question for froghopper jumping is how the azimuth is controlled. We have therefore analysed how the forces in the coxo-trochanteral joints are likely to be delivered to the ground by the mechanics of the hind legs. The mechanics suggests two possible mechanisms of azimuth control: one in which it is determined by the initial placement of the hind tibiae, and a second in which it is controlled by the amount of delay between the propulsive movements of the two hind legs. Predictions from this analysis were then tested using high-speed imaging of the natural jumping performance before and after experimental interventions. We show that the azimuth of the jump is controlled by initial placement of the metathoracic tibiae, which thus determine the vector of the thrust that propels jumping.

MATERIALS AND METHODS

To analyse leg positions and the subsequent jump trajectories, adult froghoppers, *Philaenus spumarius* (Linnaeus 1758), were caught near Cambridge, UK. They belong to the order Hemiptera, sub-order Auchenorrhyncha and to the family Cercopidae. To analyse the detailed movements of the hind legs during natural jumping, individuals were allowed to jump from a glass slide coated with a thin layer of transparent Sylgard (Dow Corning, Midland, MI, USA) to provide a good purchase for the legs. When jumping on an uncoated glass slide, both hind legs slipped so that they were unable to propel an effective jump. Images of jumping, which occurred spontaneously or was elicited by a light touch with a fine paintbrush, were captured from a ventral perspective at a rate of 5000 frames s^{-1} and an exposure time of 0.04 ms, with a Photron Fastcam 1024 PCI camera [Photron (Europe) Ltd, Marlow, Bucks., UK]. The positions of the hind legs, angular movements, and jump trajectories were measured in 23 natural jumps by 23 froghoppers. The azimuth of each tibia was measured by using the femoro-tibial joint and the distal end of the tibia as landmarks. The orientation of the body was measured by using the anterior tip of the head and the posterior tip of the abdomen as landmarks. The jump trajectory was measured by passing a line through the centre of mass in each successive image. The angular velocity was measured by recording the yaw of the body in each image, and taking the mean angular velocity over five successive images.

To determine whether there were any differences in the timing of the left and right hind legs during natural jumping, we analysed jumps from three species of froghopper that all share the same mechanism of jumping (Burrows, 2006a); *Philaenus spumarius*, *Aphrophora alni* (Fallén 1805) and *Cercopis vulnerata* (Rossi 1807). The latter two species were also caught near Cambridge, UK. The jumps occurred from either a substrate of high density foam, and were viewed from the side, or from transparent Sylgard, and were viewed ventrally. The analysis was then extended to 157 restrained jumps by 15, *Aphrophora alni*. Each froghopper was mounted ventral side up in Plasticine so that the hind legs were able to move freely. The sequence of rapid movements of both hind legs in these restrained froghoppers closely resemble those used in natural jumping (Burrows, 2006b). The movements of the proximal joints of the hind legs were viewed ventrally by mounting the Photron camera on a Leica MZ16 stereo microscope. Images were captured at rates of 30,000 frames s^{-1} and with an exposure time of 0.02 ms. This second and larger species of froghopper was used here because it was less prone to desiccation under the bright lights needed at these very high frame rates. Images from all experiments were fed directly to a computer and analysed with CorelDraw 11 (Ottawa, Canada) to determine the kinematics.

To estimate the effect of only one hind leg propelling a jump, we captured images of 13 jumps by 13 *Philaenus*. In seven of them, the left hind tibia was removed at the femoro-tibial joint, and in the other six the right hind tibia was removed. Jump trajectories in the azimuth plane that were parallel to the midline of the body were assigned a value of zero; those toward the side of the intact hind leg were assigned positive values, and those toward the side with the missing tibia were assigned negative values. Take-off time was designated as 0 ms. Data are given as mean ± standard deviation (s.d.).

To estimate the effects on the final jump trajectory of differences in the timing of the movements of the left and right hind legs, and independently, their different placements, we built a kinetic model (details in Appendix) that approximated a froghopper (parameters based on *Aphrophora alni*) as linkages each powered by a spring (Fig. 1). The model was built in Mathematica, and the equations were solved using a Runge–Kutta integrator with a timestep of 5 μs.

RESULTS

Physical constraints on jumping by froghoppers

Jumping is powered by the prolonged contractions of huge trochanteral depressor muscles in the metathorax which occur while the hind legs are locked in their fully levated positions (Burrows, 2006b; Burrows, 2007c). The energy developed by their contractions bends two bilaterally symmetrical pleural arches that link the ventral articulation of each hind coxa about the thorax to the dorsal articulation of the ipsilateral hind wing with the thorax (Fig. 1A,B). When the hind legs are unlocked, the simultaneous recoil of the pleural arches generates a large torque about each coxo-trochanteral joint (τ_L and τ_R; Fig. 1C,D). This in turn places strong torques on the hind femora and the body (Fig. 1B–D), but there is little muscle mass spanning the femoro-tibial joints to transmit this torque to the tibiae (Fig. 1E). Consequently, a hind tibia has no net torque on it, and because it is light and represents less than 1% of the body mass (Burrows, 2006b) its moment of inertia is also negligible. A consequence is that the lateral (l) and anterior (a) components of the ground (**G**) reaction force ($\mathbf{G}_l$, $\mathbf{G}_a$) of a hind leg must also produce zero torque about the femoro-tibial joint (Fig. 1E):

$$\mathbf{G}_{Ra}\, Length_{ti} \sin(\theta_{Rti}) - \mathbf{G}_{Rl}\, Length_{ti} \cos(\theta_{Rti}) = 0, \quad (1)$$

which simplifies to:

$$\mathbf{G}_{Rl} / \mathbf{G}_{Ra} = \tan(\theta_{Rti}). \quad (2)$$

The ground reaction force generated by one hind leg is therefore in a direction parallel to the longitudinal axis of the tibia of that leg. For example, a jump powered solely by depression of the left trochanter should produce a ground reaction force parallel to the left tibia. In natural jumping, if both tibiae were placed symmetrically and both coxo-trochanteral joints were depressed synchronously, then the lateral components of the forces of the two tibiae will be equal and opposite, producing a trajectory with no azimuth. If, however, the froghopper were to place its tibiae asymmetrically relative to the midline of its body, the body trajectory should be predicted by the average of the angles subtended by each tibia relative to the midline (θ_{Rti}, θ_{Lti}; Fig. 1B).

Because the force vector from each hind leg acts from the point of ground contact and is parallel to that leg, the ground reaction force cannot generate a vector that goes through the centre of mass of the body: one hind leg acting on its own should cause the body to spin. The only way for a hind leg not to generate a torque would be for its tibia to be pointed at the centre of mass, a physiologically difficult position for the froghopper to adopt. The left hind leg thus

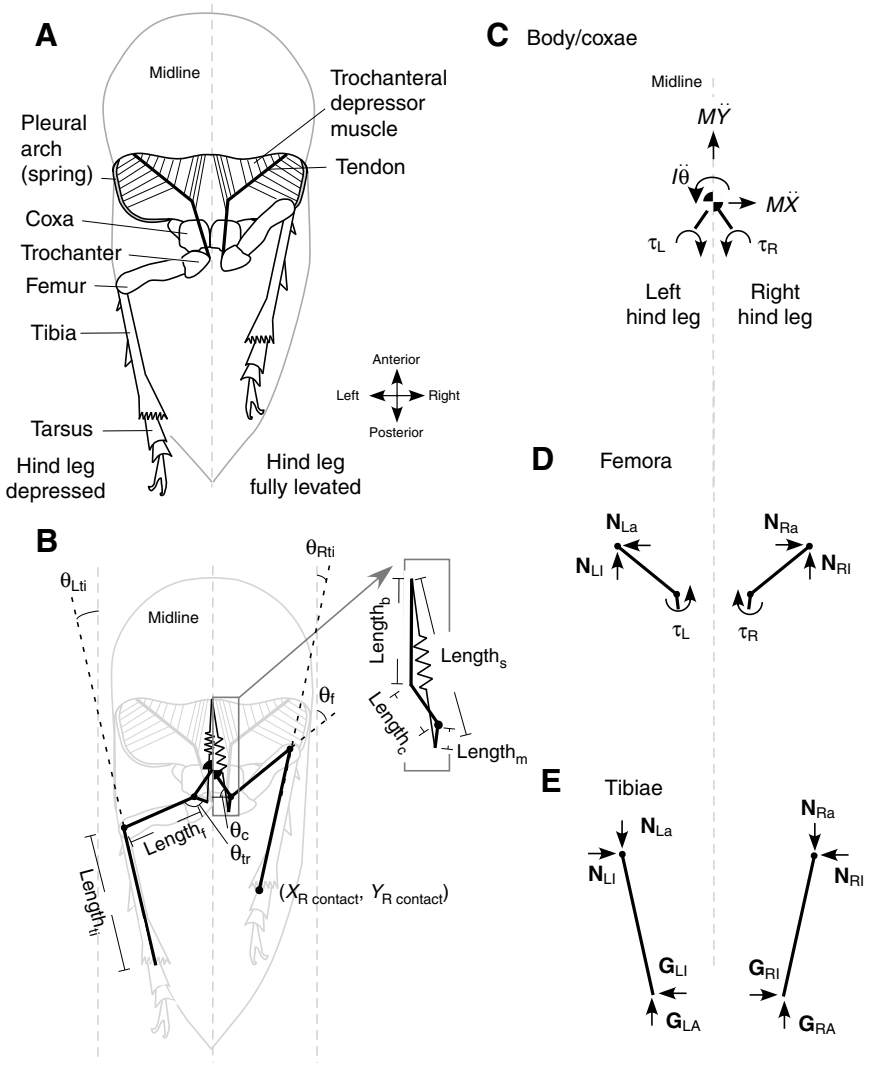

Fig. 1. Anatomy and mechanical arrangements of froghopper hind legs. (A) Anatomical sketch of a froghopper viewed ventrally to show the trochanteral depressor muscles in the metathorax and hind legs that propel jumping. The hind leg on the left is depressed and on the right is levated. (B) Mechanical schematic superimposed on the anatomical sketch to indicate the key parameters analysed. The femur and trochanter are represented by one rigid link. Inset shows an expanded view of the links between body, coxa and femur on the right side and the springs that are formal representations of the elasticity of the pleural arches that power the jump and the model (Appendix). Each arch attaches at a distance, $Length_b$, from a thoraco-coxal joint. (C–E) Free body diagrams of the body and left and right hind coxae (C), the hind femora (D) and the hind tibiae (E).

generates a clockwise torque on the body and the right leg an anti-clockwise torque. If both tibiae adopt symmetrical angles relative to the midline and both coxo-trochanteral joints are depressed synchronously, then they would generate equal and opposite torques on the body with the consequence that the body should not spin once airborne. If, however, the two coxo-trochanteral joints do not depress at the same time, the body should rotate after take-off.

Adjusting the angles adopted by the femoro-tibial joints and hence the placement of the hind tarsi on the ground before a jump would therefore be a mechanism that a froghopper could use to control the azimuth of a jump to the left or right of the body midline. Alternatively, it could also control azimuth by extending the hind legs at different times during a jump.

This analysis makes four testable predictions. (1) Symmetric placement of the hind tibiae and synchronous extension of both hind coxo-trochanteral joints should generate jump trajectories along the longitudinal axis of the body accompanied by only small amounts of body spin. (2) The azimuth of a jump should be predicted by the initial angles of the hind tibiae relative to the midline of the body; a jump should be toward the side to which the tibiae point. (3) The azimuth of a jump in which only one hind leg participates should be parallel to the tibia of that leg, and be accompanied by spin of the body in the yaw plane. A correlate of this prediction is that a jump powered by the left hind leg should rotate clockwise while a jump powered by the right hind leg should rotate anti-clockwise. (4) Adjusting the times at which the two hind legs depress could be an alternative or additional mechanism for determining the azimuth direction of a jump.

To test these predictions we therefore analysed the kinematics of natural jumping as revealed by high speed imaging.

Positioning of the hind legs before a natural jump

Prior to a jump, does a froghopper adopt a stereotyped posture, or does it adjust its posture and position of its hind legs? To determine the initial position of the hind legs, we analysed high-speed videos of natural jumps by the froghopper, *Philaenus spumarius*. Before a natural jump, a protrusion on a dorsal femur engaged with a protrusion of a coxa effectively locking the femur relative to the body (Fig. 2) (Burrows, 2006b). The result was that, prior to a jump, a froghopper could not change the angle between a femur and the longitudinal axis of the body (θ_f in Fig. 1B) and the angle between a trochanter and a femur (θ_{tr} in Fig. 1B). In the jumps analysed here, θ_f was 28±11.2 deg., but θ_{tr} was not measurable from the data here, but is about 150 deg. (Burrows, 2006b). The femoro-tibial joint is not locked, allowing a froghopper to adjust the angle of the tibiae and hence the placement of the tarsi on the ground either symmetrically or asymmetrically relative to the longitudinal midline (Fig. 3).

For a jump in which a froghopper initially placed its hind tibiae symmetrically about the longitudinal axis of the body and thus the

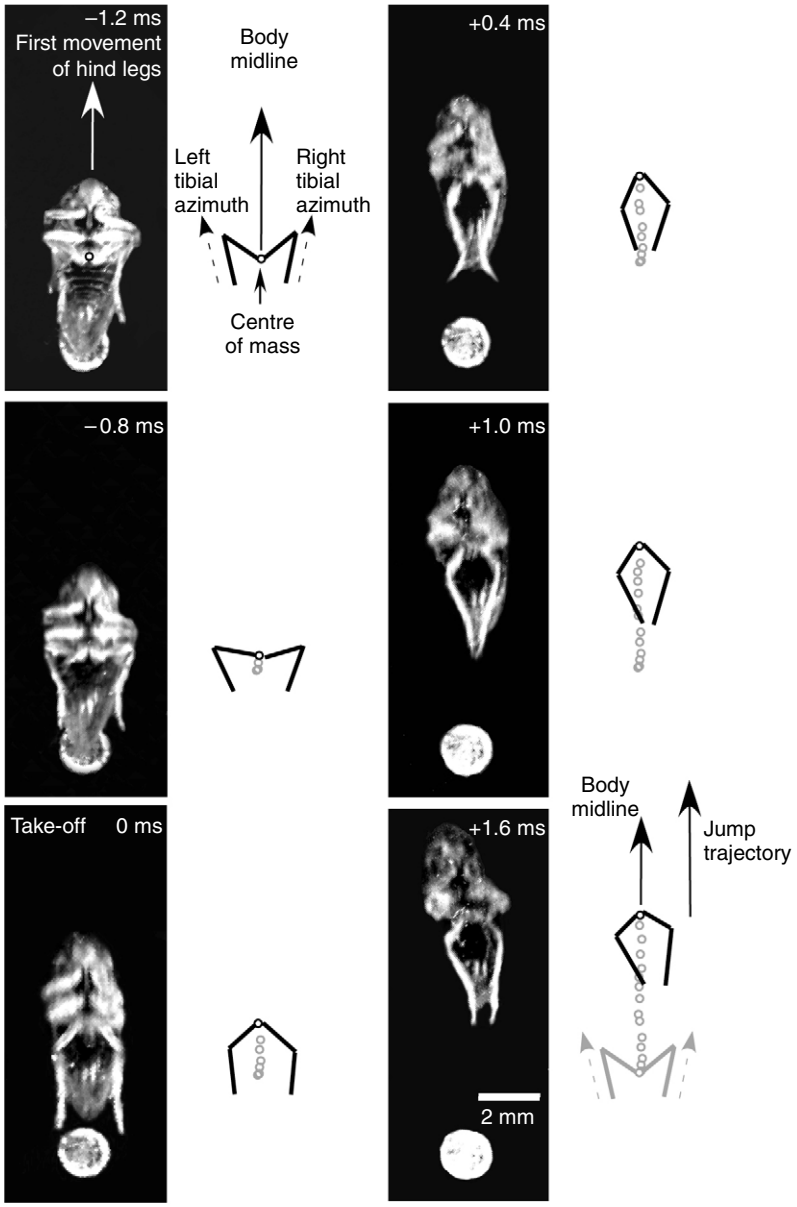

Fig. 2. Jump by the froghopper *Philaenus spumarius* viewed ventrally and captured at a rate of 5000 frames s^{-1}. Selected images are arranged in two columns and the diagrams to the right of each show the positions of the hind femora and tibiae. The centre of mass is marked with a black circle on the first image. In the second (–0.8 ms) and subsequent diagrams the positions of the centre of mass in previous images are also marked (grey circles). The midline of the body and the initial tibial positions are marked with solid and dashed arrows, respectively. The final jump trajectory is shown with a solid arrow in the last frame with previous positions in grey. The large white circle toward the bottom of each image is a fixed reference point.

tarsi symmetrically on the ground, the following sequence of movements occurred. As the trochantera and femora began to depress at the start of a jump, the effect was to push each femoro-tibial joint more laterally (Fig. 2). The tarsi remained at the same positions on the ground so that the femoro-tibial joints were extended and the front of the body was accelerated and raised from the ground. As the depression of the trochantera continued, the positions of both femoro-tibial joints now moved medially and the femoro-tibial angles were further extended. This meant that the line of action of each tibia changed continuously as the hind legs accelerated the body. At take-off both tibiae were parallel to the long axis of the body and once airborne the body was accelerated with 22 Hz of rotation in the yaw plane (Fig. 2). The implication is that the extension of the tibiae resulted from the forces applied to depress the trochanter, rather than from a contraction by the extensor tibiae muscle.

Before a jump, the net azimuth angles adopted by the tibiae of the left and right hind legs ranged from –30 to 40° (Fig. 3). The femoro-tibial angles adopted by a left and a right hind leg could be varied independently and were only weakly correlated with each other (R^2=0.22).

The azimuth trajectory of most jumps varied over a window of 60 deg., some 30 deg. to the left and right of either side of the longitudinal axis of the body (Fig. 4). The final azimuth of a jump was correlated with the mean initial azimuth of the two hind tibiae (R^2=0.68, slope=1.29, *y*-axis intercept=–0.05 deg.). If the initial mean azimuth of the tibiae was positive (they pointed to the right) then the jump azimuth was to the right, and if the initial mean azimuth of the tibiae was negative (they pointed to the left), then the jump azimuth was to the left. This indicates that trajectory is largely explained by the average of the two starting, tibial azimuths.

Synchrony of hind leg movements during jumping

To test how closely coupled the movements of the two hind legs were during natural jumping, high speed images were analysed. The jumps occurred from either a substrate of high density foam, and were viewed from the side, or from transparent Sylgard, and were

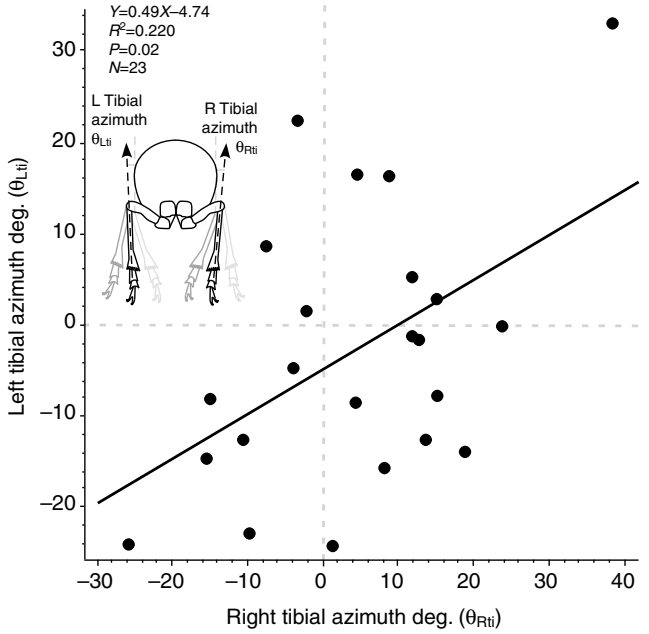

Fig. 3. Plot of the azimuth of the left and right hind tibiae at the start of the propulsive phase of 23 jumps by 23 *Philaenus spumarius*. The inset shows a sketch (ventral view and with anterior at the top) of the positions of the hind legs at the mean tibia positions (black), mean plus one standard deviation (dark grey), and mean minus one standard deviation (light grey). The values are: right hind leg 4.0±14.6 deg., left hind leg –2.8±15.0 deg.

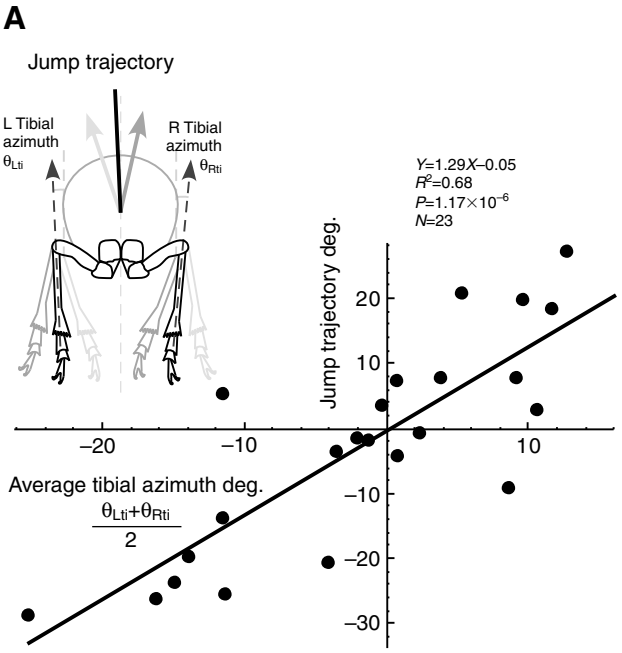

Fig. 4. A The trajectory of a jump, measured at take-off, plotted against the initial azimuth of the left and right hind tibiae. The data are from 23 jumps by 23 *Philaenus spumarius*. The inset diagram shows the mean jump azimuth (black), mean plus one standard deviation (dark grey), and mean minus one standard deviation (light grey) superimposed on a sketch of the hind legs viewed ventrally and with anterior at the top. The azimuth values are –2.4±16.3 deg.

viewed ventrally. We analysed jumps from three species of froghopper all of which have the same jumping mechanisms (Burrows, 2006a); 48 jumps from 30 *Philaenus spumarius,* 41 jumps from 8 *Aphrophora alni*, and 35 jumps from 7 *Cercopis vulnerata*. This includes 33 jumps from a previous investigation by Burrows (Burrows, 2006a) in which the hind legs on both sides could be clearly seen, and which were conducted using the same methods as used here. In 123 of these 124 jumps no difference could be detected in the start of the depression movements of the hind legs.

To test whether any differences in the timing of the two hind legs may have been masked in natural jumping by having to lift the weight of the body, jumping movements were induced in *Aphrophora alni* restrained on their backs in Plasticine, but with the hind legs free to move. Both hind legs would then kick rapidly against the resistance of only the air in a sequence of movements that closely resembled those used in natural jumping. Images of these restrained jumps were captured at 30,000 frames s^{-1}. In 157 jumps by 15 *Aphrophora*, the mean difference between the start of trochanteral depression in the two hind legs was 0.032±0.022 ms (mode and median 0.033 ms or 1 frame), and was never greater than 0.067 ms (2 frames).

In the absence of an experimental method that could manipulate the timing of the movements of the two hind legs to these levels of resolution, we used a model (Appendix) to quantify the effects of leg asynchrony on the final jump trajectory. The values modelled extended from the small measured values (Fig. 5A, vertical grey bar) in restrained jumps to the total acceleration time (2 ms) of a jump propelled by one hind leg. A jump propelled by one hind leg has half the force of a jump propelled by both hind legs, so that it takes twice as long for the hind leg to depress fully. The modelling showed that the largest measured difference in timing (67 μs) would produce an azimuth offset from the longitudinal midline of only 0.4 deg. (Fig. 5A). With an asynchrony of 2 ms, the jump azimuth was increased to 14 deg. By contrast, using asymmetrical tibial positions within the range observed in natural jumping and making the tibiae depress symmetrically, the model could produce the full range of observed azimuths (up to 25 deg.; Fig. 4, Fig. 5A).

The angular velocity of simulated jumps increased as timing differences were increased, reaching 77 Hz at 2 ms of asynchrony (Fig. 5B). By contrast, changing tibial positions while both hind legs moved at the same time resulted in a spin of no more than 5 Hz, or 6% of that experienced with a 2 ms timing difference (Fig. 5B).

The simulations also show that controlling azimuth with asynchronous movements of the hind legs is energetically inefficient. The kinetic energy ($1/2mV^2$) dropped from 88 μJ, when the hind leg movements were synchronous, to 29 μJ (a 67% decrease) when one leg was depressed 2 ms after the other (Fig. 5C). By contrast, if azimuth was changed by adjusting the initial position of the hind tibiae then the kinetic energy remained constant. This is because moving the hind legs asynchronously causes two losses of energy. First, asynchronous jumps have less kinetic energy because the leg moving last will not initially be in contact with the ground and thus does not transmit its force directly to the ground. Second, asynchrony generates body spin and a loss to rotation of as much as 17% of the energy. By contrast, jumps powered by synchronous movements of the hind legs lose only about 1% of energy to spin. The projected take-off velocity of a jump also fell from 2.5 m s^{-1} when the hind legs moved synchronously to 1.4 m s^{-1} when they moved asynchronously. The fall resulted from a loss of energy due to spin and from a reduction in the total energy available.

Jumping propelled by one hind leg

In only one of the 124 natural jumps analysed was one hind leg seen to depress before the other (Fig. 6), emphasising the rarity of such events. In this jump the left hind leg moved 1 ms before the right hind leg which caused the body to rotate before the right leg could make any contribution. As predicted from the modelling above, the movement of the left hind leg caused a fast clockwise rotation (78 Hz). Furthermore, the time to take-off was 2.2 ms or about twice that taken when a jump was propelled by two hind legs depressing synchronously.

To obtain more experimental data on how the azimuth is controlled in jumps propelled by one hind leg, we removed the left hind tibia in one group of seven *Philaenus* and the right tibia in another group of six, and then correlated the initial position of the remaining tibia with the resulting azimuth at take-off (Fig. 7, Fig. 8A). Jumps powered by one hind leg generated trajectories that were linearly related (slope=1.15, R^2=0.66) to the initial azimuth of the sole remaining tibia (Fig. 8A). In 8 of the 13 jumps analysed the trajectory was toward the side of the functional hind leg. The trajectory of a jump powered by one hind leg was thus largely explained by the starting azimuth of the tibia. All 13 jumps powered by one hind leg were accompanied by rotation rates of 161±55.7 Hz (N=13) compared with rotation rates of 28±23.6 Hz (N=23) when jumps were propelled by both hind legs (Fig. 8B). For jumps powered only by the left hind leg the spin was clockwise and for jumps powered only by the right hind leg it was anti-clockwise.

DISCUSSION

Froghoppers control the azimuth of their jumps by altering the angles of the left and right hind tibiae relative to the midline of their body and then synchronously and rapidly depressing both hind trochantera. The mean angle of the two hind tibiae determines the azimuth of a jump which can deviate from the longitudinal axis of the body by about ±30 deg. Images of natural and experimentally manipulated jumps show that the azimuth is strongly correlated with the initial position of the hind tibiae, and kinetic modelling has shown how this happens and why it is an energetically favourable method to control azimuth.

To jump, a froghopper uses huge muscles in the thorax to generate large torques on both the thorax and the trochantera. The torque is not, however, transmitted to the tibiae because the muscles moving the femoro-tibial joints are small. A consequence of this arrangement is that the ground reaction force generated by one hind leg is parallel to the longitudinal axis of its tibia. This means that if both hind tibiae are placed symmetrically and both coxo-trochanteral joints depress synchronously, then the lateral components of the forces generated by the left and right hind legs will be equal and opposite, and the azimuth of a jump will be parallel to the long axis of the body. If, however, the hind tibiae are placed asymmetrically, the trajectory of a jump is determined by the average of the angles subtended by each tibia relative to the midline. During natural jumping the mean, initial tibial angles of both hind legs and the azimuth of a resulting jump are strongly correlated. It follows that in froghoppers with only one hind leg, the azimuth of a jump will be determined by the angle of the remaining tibia. An undesirable consequence of using just one hind leg is that the body now spins on average six times faster than when powered by both hind legs, dissipating enormous amounts of energy and resulting in less effective jumps. This may explain why froghoppers with just one hind leg are rarely found in nature.

Modelling indicates that jump azimuth could theoretically be controlled by extending the hind legs asynchronously, but analysis of froghoppers executing restrained jumps reveals a remarkable synchrony in the movements of both hind legs (mean timing difference of only 32 µs). Furthermore, in only one of 124 natural jumps analysed was the timing difference visible. This means that

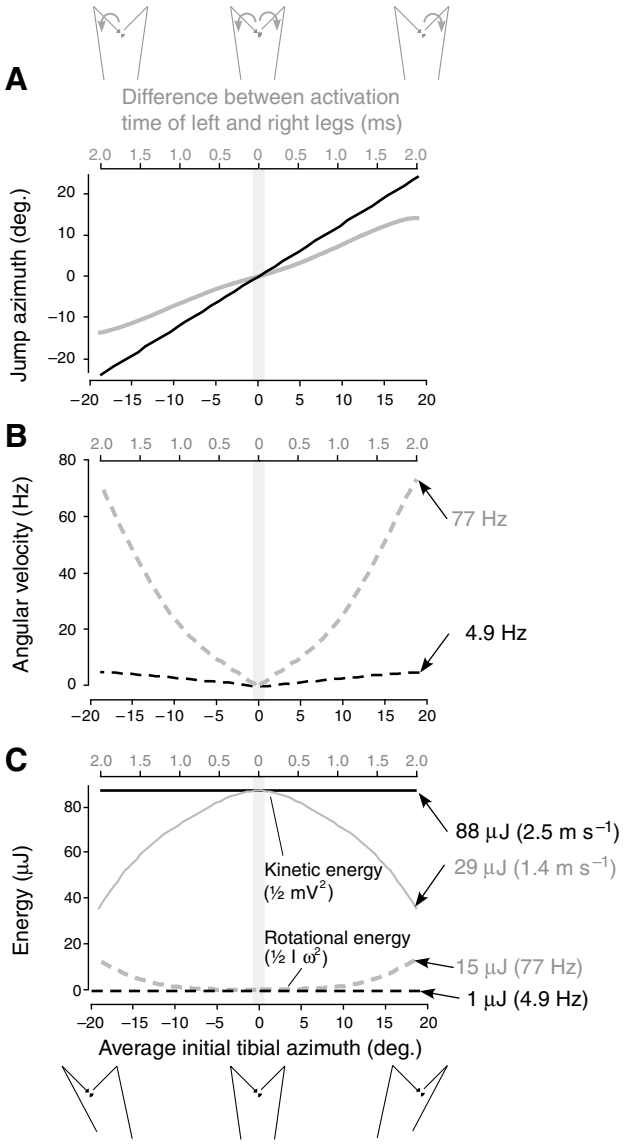

Fig. 5. Model simulations of jumping performance: (A) jump azimuth; (B) jump velocity and rotation; (C) jump energy. Each graph was generated by changing either the initial positions of the left and right hind tibiae (black lines), or the timing differences between the movements of the left and right hind legs (grey lines). The vertical grey bar in all graphs marks the observed maximum asynchrony (67 µs) of hind leg movements in *Aphrophora alni*. (A) Jump azimuth. By changing the initial position of the tibiae (black) the model was able to generate the whole range of observed azimuths. By contrast, the model was only able to generate most of the range of observed azimuths if the asynchrony between the legs was increased to values not observed in natural jumping. (B) Jump rotation rates. Controlling azimuth with leg asynchrony causes higher rates of spin (grey) compared with controlling it by changing the initial positions of the hind tibiae (black). (C) Jump energy. Energy in translation ($1/2\,mV^2$) is shown by solid lines, and in rotation ($1/2\,I\omega^2$) by the dashed lines. Arrows indicate the values at timing differences of 2 ms. The high rate of spin caused by controlling azimuth with hind leg asynchrony causes a large energy sink (grey), but controlling azimuth by adjusting the initial tibial positions (black) results in only a small energy loss.

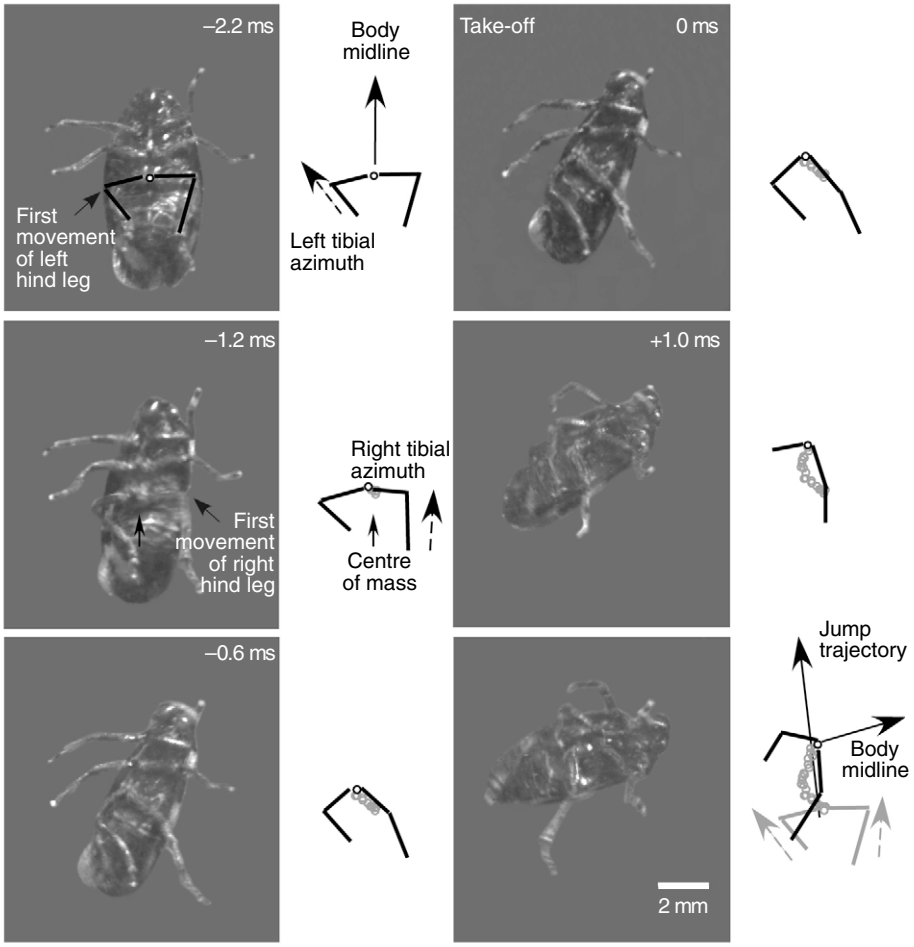

Fig. 6. A rare asynchronous depression of the hind legs powering a natural jump by *Cercopis vulnerata* caused the body to spin. Images, at the times indicated, were captured at a rate of 5000 frames s^{-1}. The left femur depressed first at –2.2 ms but the depression of the right femur did not start until –1.2 ms, by which time the movement of the left hind leg had already caused the body to rotate. The bottom left hand corner of each frame is a fixed reference point.

if the tibia are placed symmetrically and both legs are synchronously depressed, then the azimuth of the jump will be parallel to the longitudinal axis of the body. There are severe limitations if the froghopper attempts to control azimuth by adjusting the timing differences between the movements of its hind legs. First, the largest (67 μs) difference in timing observed in natural jumping would only contribute some 0.4 deg. to azimuth control. Second, modelling shows that increasing the time differences up to the 1 ms of the acceleration period for a natural jump, can achieve greater azimuth control but only at the expense of progressively increasing body spin and energy losses that would substantially degrade take-off velocity. As timing differences increase past that point, the jump essentially becomes powered by just one hind leg so that the trajectory is determined by the tibial angle of that leg and high rates of body spin are unavoidable.

These results may explain why froghoppers so rarely depress their two legs asynchronously when jumping. They may also explain the requirement for controlling the power producing muscles on the two sides of the body with closely synchronised sequences of motor spikes (Bräunig and Burrows, 2008; Burrows, 2007c). Synchrony of the motor spikes to the left and right muscles is likely to produce closely matching levels of force in each and increase the probability that both hind legs will move at the same time. Controlling azimuth by adjusting the timing of the movements of the two hind legs to within a fraction of a millisecond would, however, still be a challenging task for neural control. Instead, changing the initial position of the tibiae is both a simpler and more energetically efficient mechanism.

How accurately do tibial angles predict jump azimuth?

The azimuth of a jump by a froghopper is strongly correlated with the initial azimuth of the tibiae; for natural jumps powered by both hind legs the slope of the relationship was 1.29 and for experimental jumps powered by a single hind leg it was 1.15. If the force vector was perfectly parallel to the tibia, the slope should be 1 for both data sets. What is the cause of the small discrepancies? The calculations were simplified by making three assumptions. First, we assumed that the angle of a tibia relative to the midline remains constant during a jump. High speed images of the hind leg movements clearly show, however, that the depression of the trochantera and femora (resulting from the release of stored energy in the pleural arches) cause the azimuth of the tibiae to change continuously during the acceleration phase of a jump (Fig. 2) (Burrows, 2006a). As the coxo-trochanteral joints depress, the femoro-tibial joints are forced laterally, thus increasing the angle of the tibiae relative to the longitudinal axis of the body. Continuing depression then causes the femoro-tibial joints to move medially, decreasing the angle. These changing orientations of the tibiae mean that their force vectors also change progressively. Second, we assumed that the magnitude of force vectors of the tibiae were constant throughout a jump. In fact they will change as the springs of the pleural arches progressively recoil. Third, no torque was assumed to be transmitted through the femoro-tibial joints, but some may be. The calculations made here take no account of these three factors and yet initial positions of the tibiae alone predict linear intercepts of 0 deg. when plotted against jump azimuth. The experimental data show intercepts of 0.05 deg. and 2.16 deg. for two-

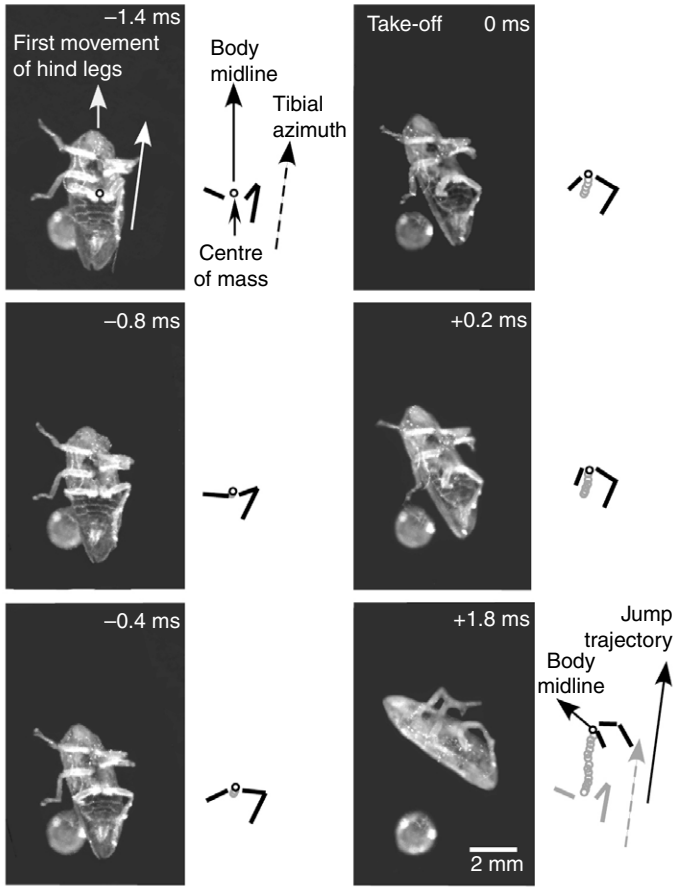

Fig. 7. A jump by *Philaenus spumarius* with the hind tibia removed has a trajectory that follows the azimuth of the remaining right hind tibia. Images, at the times indicated, and captured at a rate of 5 000 frames s^{-1} are displayed in two columns. The diagrams to the right indicate the positions of the two hind femora, but only the right hind tibia. The grey circle represents a fixed reference point in each frame.

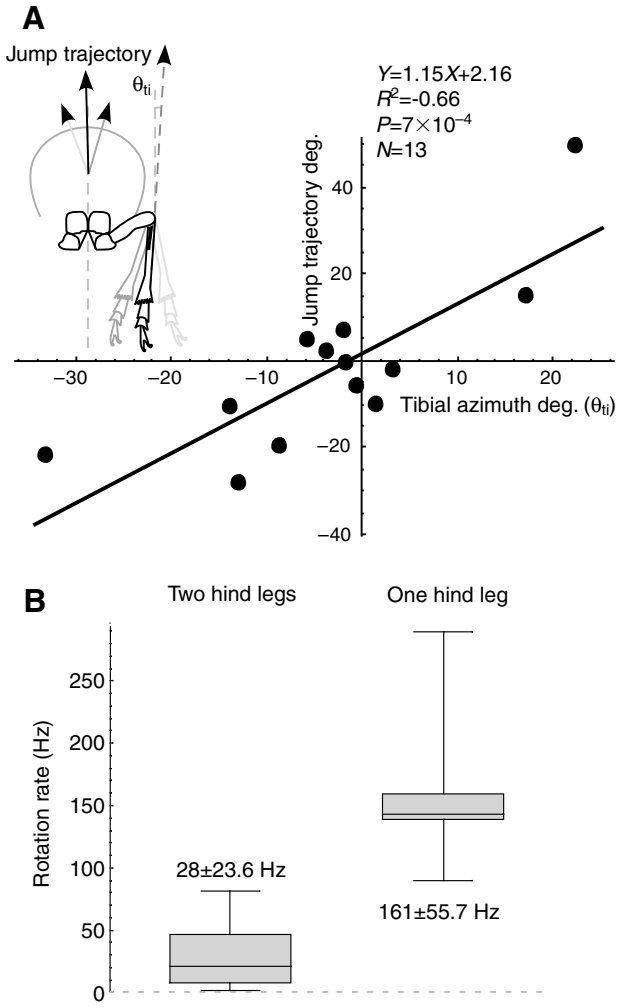

Fig. 8. Trajectories of jumps propelled by one hind leg. (A) Jump azimuth at take-off plotted against initial azimuth of the remaining hind tibia. The data are from 13 jumps by 13 *Philaenus spumarius*. The inset sketch shows the mean jump trajectory (black) and the mean tibial azimuth (black), the mean plus one standard deviation (dark grey), and the mean minus one standard deviation (light grey). The value for the jump azimuth is –1.3±19.5 deg. The value for leg azimuth is –3±13.8 deg. (B) Box and whisker plot of the rates of rotation for 23 jumps propelled by both hind legs (left), and for 13 jumps propelled by one hind leg (right).

legged and one-legged jumps, respectively, that are thus close to the expected value given the simplifying assumptions made. A more accurate predictor could be developed from the diagrams in Fig. 1 but this would require, for only a very small gain, detailed, real-time measurements of the stiffness and forces delivered by each pleural arch, of changes in moment arms of the trochantera and moment of inertia of the froghopper, and ground forces, or three-dimensional measurements of the kinematics to determine kinetic energy (both in translation and in rotation).

Implications of this strategy on the resolution of jump control

Brackenbury (Brackenbury, 1996) found that froghoppers and leafhoppers could jump to targets with a resolution of 7 deg. × 7 deg., and suggested that the constraints on the targeting were due to both visual and biomechanical factors. In terms of jump azimuth, however, we find no evidence to support a biomechanical limit on the resolution of a jump because trajectories of a jump are controlled by adjusting the initial positions of the hind tibiae. This suggests that the limitations are a consequence of the sensory system which are discussed by Brackenbury (Brackenbury, 1996).

Is this control strategy used by other insects?

The strategy proposed here for controlling azimuth should apply to insects that have: (1) jumps propelled by legs that move in the same plane; (2) jumps that are powered by muscles that move the coxo-trochanteral joint; (3) leg segments that remain approximately rigid during a jump and do not bend.

Leafhoppers (Burrows, 2007a; Burrows, 2007b; Burrows and Sutton, 2008) and possibly members of some of the other families in the Auchenorrhyncha meet these criteria and could thus be tested experimentally to see if their control of azimuth is the same. In *Hackeriella* (Hemiptera, Coleorrhyncha) the hind legs that propel jumping are also slung beneath the body but can propel jumps with greater asynchrony than that seen in either frog- or leafhoppers (Burrows et al., 2007). Fleas propel jumping with muscles that act at the coxo-trochanteral joints of the hind legs (Bennet-Clark and Lucey, 1967) like a froghopper, but have their legs placed at the sides of their bodies like a locust. It is not known how they control the direction of their jumping.

A different jumping strategy in Orthoptera

The strategies for jumping in froghoppers and orthopterans such as grasshoppers and locusts appear to be distinct. First, locusts generate the forces required for jumping by contractions of muscles that move the femoro-tibial joints of the hind legs. Second, the hind legs move in separate planes to each other on either side of the body. This arrangement means that the force vectors that propel a locust jump remain in a constant direction that is determined at the joint between the coxa and the fused trochanter and femur. Rotations of as much as 90 deg. at this joint set the angle of elevation for a jump (Sutton and Burrows, 2008), in contrast to a froghopper where elevation is set by movements of the front and middle legs. Consequently, a locust, which experiences neither changes in the direction of force vectors as its hind legs move, nor an intrinsic torque on the body caused by those vectors, does not have to balance the forces between the two hind legs. It therefore has no difficulty jumping with just one hind leg, or when both hind legs extend with some delay between them (Bennet-Clark, 1975; Santer et al., 2005; Sutton and Burrows, 2008). This is in contrast to the froghopper, which experiences changing force directions and intrinsic torques on the body as it hind legs depress synchronously. Azimuth in froghoppers is controlled by the positions of the hind tibiae, whereas in grasshoppers it is controlled by the front legs shifting the orientation of the whole body (Santer et al., 2005).

Despite the differences in strategies, the jumping by both froghoppers and grasshoppers illustrate common underlying principles. In both, control of three key parameters, velocity, elevation and azimuth, are compartmentalised. Velocity is controlled by the force generated at the coxo-trochanteral joints of froghoppers (Burrows, 2007c; Burrows et al., 2008) and at the femoro-tibial joints of grasshoppers (Bennet-Clark, 1975). Elevation is controlled by the front and middle legs of froghoppers (Burrows, 2006a) and at the hind coxo-femoral joints in grasshoppers (Sutton and Burrows, 2008). Finally, azimuth is controlled at the femoro-tibial joints in froghoppers and by the front legs in grasshoppers (Santer et al., 2005). The separation of these functions, albeit in different joints or legs, should allow a simpler neural control with each parameter being set independently once a target has been identified.

Easily directed trajectories appear to be common in high speed motions. The controllability of the jumping movements described have parallels with the tongue strike of a toad (Mallett et al., 2001), the strike of a squid tentacle (Van Leeuwen and Kier, 1997) and suction feeding (Van Wassenbergh and Aerts, 2009; Wainwright et al., 2007) in which there is a simple transformation from the initial position to the final trajectory. Ease of control of high speed motions allows a nervous system to prepare, in real time, controlled motions quickly and easily in response to visual or tactile stimuli (Card and Dickinson, 2008).

Further analyses of the strikes of mantid shrimps (Burrows, 1969; Patek and Caldwell, 2005), praying mantids (Gray and Mill, 1983) and snakes (Smith et al., 2002) would usefully reveal whether they are also mechanically configured to produce easily controlled trajectories. High-speed motions represent a clear example where the biomechanics and the neural control work together to generate successful behaviours both for predators and for prey (Chiel and Beer, 1997; Dickinson et al., 2000).

APPENDIX

The equation of motion for the froghopper model is based on the same assumptions that were used for modelling the control of elevation in jumping of locusts (Sutton and Burrows, 2008). The following assumptions were made about a froghopper. The hind legs are small relative to the size of the body (Burrows, 2006a; Burrows, 2006b), so that the femora and tibiae were assumed to have no mass. The leg segments do not appear to bend during a jump (Burrows, 2006b), allowing the coxa, femur and tibia to be modelled as rigid bodies. The trochanter moves with the femur during a jump (Burrows, 2006b), allowing it to be modelled as a part of the femur. The body of the froghopper was assumed to be a uniform disk (model parameters in Table A1).

Based on these assumptions and the data from free-body diagrams of a froghopper (Fig. 1) nine equations were derived to calculate the accelerations ($\ddot{X}$, $\ddot{Y}$, $\ddot{Z}$) in terms of joint torques (τ_L, τ_R):

The free body diagram (Fig. 1C–E) yielded the accelerations of a froghopper ($\ddot{X}$, $\ddot{Y}$, $\ddot{Z}$) in terms of the ground reaction forces ($\mathbf{G}_{La}$, $\mathbf{G}_{Ll}$, $\mathbf{G}_{Ra}$, $\mathbf{G}_{Rl}$):

$$M\ddot{Y} = \mathbf{G}_{La} + \mathbf{G}_{Ra} \quad \text{(A1)}$$

$$M\ddot{X} = \mathbf{G}_{Ll} + \mathbf{G}_{Rl} \quad \text{(A2)}$$

$$\begin{aligned} I\ddot{\theta} = {} & \mathbf{G}_{La}\,(Length_f \sin(\theta_{Lf}) - Length_t \sin(\theta_{Lti}) - Length_c \cos(\theta_{Lc})) \\ & - \mathbf{G}_{Ll}\,(-Length_f \cos(\theta_{Lf}) + Length_t \cos(\theta_{Lti}) + Length_c \cos(\theta_{Lc})) \\ & + \mathbf{G}_{Ra}\,(Length_f \sin(\theta_{Rf}) - Length_t \sin(\theta_{Rti}) + Length_c \cos(\theta_{Rc})) \\ & + \mathbf{G}_{Rl}\,(Length_f \cos(\theta_{Rf}) + Length_t \cos(\theta_{Rti}) + Length_c \sin(\theta_{Rc}))\,. \end{aligned} \quad \text{(A3)}$$

The forces are in terms of lateral (l) and anterior (a) components, and the femoral and tibial angles are defined relative to the midline of the froghopper.

Table A1. Model parameters

Parameter name	Value	Source
Mass (M)	28.3 mg	(Burrows, 2006a)
Tibial length ($Length_{ti}$)	2.5 mm	(Burrows, 2006a)
Femoral length ($Length_f$) (includes trochanter)	1.5 mm	(Burrows, 2006a)
Moment arm length ($Length_m$)	0.33 mm	(Burrows, 2006b)
Coxal length ($Length_c$)	0.73 mm	(Burrows, 2006b)
Distance between spring attachment and coxa ($Length_b$)	0.57 mm	Parameterized to fit spring rest length
Trochanteral angle (θ_{tr})	150 deg.	(Burrows, 2006b)
Coxal angle (θ_c)	55 deg.	(Burrows, 2006b)
Initial femoral angle (θ_f)	45 deg.	(Burrows, 2006b)
Initial tibial angle (θ_{ti})	8 deg.	Fig. 3
Spring rest length	1.1 mm	(Burrows et al., 2008)
Spring stiffness (K)	832 mN mm^{-1}	Parameterized for 44 μJ of energy per spring: (Burrows, 2006a)
Body radius (r)	3 mm	
Timestep (t)	5 μs	

The elastic recoil of the pleural arches puts a torque about the thoraco-coxal joints, so that the moments about the femoro-tibial joint can be assumed to be zero, generating the following equations by summing the torques about the femoro-tibial joints (Fig. 1E):

$$\mathbf{G}_{\mathrm{La}}\, Length_{\mathrm{ti}} \sin(\theta_{\mathrm{Lti}}) + \mathbf{G}_{\mathrm{Ll}}\, Length_{\mathrm{ti}} \cos(\theta_{\mathrm{Lti}}) = 0 \qquad \text{(A4)}$$

$$\mathbf{G}_{\mathrm{Ra}}\, Length_{\mathrm{ti}} \sin(\theta_{\mathrm{Rti}}) + \mathbf{G}_{\mathrm{Ll}}\, Length_{\mathrm{ti}} \cos(\theta_{\mathrm{Rti}}) = 0\,. \qquad \text{(A5)}$$

By summing the forces on the tibiae, and assuming the masses of the tibiae are negligible, four more equations relate the normal forces ($\mathbf{N}_{\mathrm{LX}}$, $\mathbf{N}_{\mathrm{LY}}$, $\mathbf{N}_{\mathrm{RX}}$, $\mathbf{N}_{\mathrm{RY}}$) with the ground reaction forces ($\mathbf{G}_{\mathrm{La}}$, $\mathbf{G}_{\mathrm{Ll}}$, $\mathbf{G}_{\mathrm{Ra}}$, $\mathbf{G}_{\mathrm{Rl}}$):

$$\mathbf{N}_{\mathrm{Ll}} = \mathbf{G}_{\mathrm{Ll}} \qquad \text{(A6)}$$

$$\mathbf{N}_{\mathrm{La}} = \mathbf{G}_{\mathrm{La}} \qquad \text{(A7)}$$

$$\mathbf{N}_{\mathrm{Rl}} = \mathbf{G}_{\mathrm{Rl}} \qquad \text{(A8)}$$

$$\mathbf{N}_{\mathrm{Ra}} = \mathbf{G}_{\mathrm{Ll}}\,. \qquad \text{(A9)}$$

The elastic recoil of the pleural arches puts torques about the left and right femora (τ_{L} and τ_{R}), and yields the following equations by summing the torques about the coxa-trochanteral joints (Fig. 1D):

$$\mathbf{N}_{\mathrm{Ll}}\, Length_{\mathrm{f}} \cos(\theta_{\mathrm{Lf}}) - \mathbf{N}_{\mathrm{La}}\, Length_{\mathrm{f}} \sin(\theta_{\mathrm{Lf}}) = \tau_{\mathrm{L}} \qquad \text{(A10)}$$

$$\mathbf{N}_{\mathrm{Rl}}\, Length_{\mathrm{f}} \cos(\theta_{\mathrm{Rf}}) + \mathbf{G}_{\mathrm{Ra}}\, Length_{\mathrm{f}} \sin(\theta_{\mathrm{Rf}}) = \tau_{\mathrm{R}}\,. \qquad \text{(A11)}$$

Eqns 1–11 can then be solved for the accelerations of the body ($\ddot{X}$, $\ddot{Y}$, $\ddot{\theta}$) in terms of joint torques and leg positions:

$$\ddot{Y} = \frac{-\tau_{\mathrm{L}}\cos(\theta_{\mathrm{Lti}})}{M\sin(\theta_{\mathrm{Lf}} - \theta_{\mathrm{Lti}})\,Length_{\mathrm{f}}} + \frac{\tau_{\mathrm{R}}\cos(\theta_{\mathrm{Rti}})}{M\sin(\theta_{\mathrm{Rf}} - \theta_{\mathrm{Rti}})\,Length_{\mathrm{f}}}\,, \qquad \text{(A12)}$$

$$\ddot{X} = \frac{-\tau_{\mathrm{L}}\sin(\theta_{\mathrm{Lti}})}{M\sin(\theta_{\mathrm{Lf}} - \theta_{\mathrm{Lti}})\,Length_{\mathrm{f}}} + \frac{\tau_{\mathrm{R}}\sin(\theta_{\mathrm{Rti}})}{M\sin(\theta_{\mathrm{Rf}} - \theta_{\mathrm{Rti}})\,Length_{\mathrm{f}}}\,, \qquad \text{(A13)}$$

$$\ddot{\theta} = \frac{\tau_{\mathrm{L}}(-Length_{\mathrm{f}} + Length_{\mathrm{c}}\cos(\theta_{\mathrm{c}} - \theta_{\mathrm{Lti}}))}{I\,Length_{\mathrm{f}}\sin(\theta_{\mathrm{Lf}} - \theta_{\mathrm{Lti}})} + \frac{\tau_{\mathrm{R}}(Length_{\mathrm{f}} + Length_{\mathrm{c}}\cos(\theta_{\mathrm{c}} - \theta_{\mathrm{Rti}}))}{I\,Length_{\mathrm{f}}\sin(\theta_{\mathrm{Lf}} - \theta_{\mathrm{Lti}})}\,. \qquad \text{(A14)}$$

The torques applied by each spring (the pleural arches; τ_{L}, τ_{R}) were calculated by multiplying the force in each spring by its moment arm. The force in each spring was calculated as:

$$Spring\ force = \mathrm{K}\,(Length_{\mathrm{s}} - Spring\ rest\ length)\,. \qquad \text{(A15)}$$

$Length_{\mathrm{s}}$ was determined by the angle of the femur relative to the midline of the froghopper. To generate the torques (τ_{L}, τ_{R}) generated by each spring, the force was multiplied by the perpendicular moment arm of the spring about the coxo-trochanteral (plus femur) joint.

$$\tau = Spring\ force \times Moment\ arm\,. \qquad \text{(A16)}$$

A final kinematic constraint is that, until take-off, each hind leg must connect the ground contact points with the body position (X,Y):

$$X + Length_{\mathrm{f}}\sin(\theta_{\mathrm{Rf}}) - Length_{\mathrm{ti}}\sin(\theta_{\mathrm{Rti}}) + Length_{\mathrm{c}}\cos(\theta_{\mathrm{Rc}}) = X_{\mathrm{Rcontact}} \qquad \text{(A17)}$$

$$Y + Length_{\mathrm{f}}\cos(\theta_{\mathrm{Rf}}) - Length_{\mathrm{ti}}\cos(\theta_{\mathrm{Rti}}) + Length_{\mathrm{c}}\sin(\theta_{\mathrm{Rc}}) = Y_{\mathrm{Rcontact}} \qquad \text{(A18)}$$

$$X + Length_{\mathrm{f}}\sin(\theta_{\mathrm{Lf}}) - Length_{\mathrm{ti}}\sin(\theta_{\mathrm{Lti}}) + Length_{\mathrm{c}}\cos(\theta_{\mathrm{Lc}}) = X_{\mathrm{Lcontact}} \qquad \text{(A19)}$$

$$Y + Length_{\mathrm{f}}\cos(\theta_{\mathrm{Rf}}) - Length_{\mathrm{ti}}\sin(\theta_{\mathrm{Rti}}) + Length_{\mathrm{c}}\cos(\theta_{\mathrm{Rc}}) = Y_{\mathrm{Rcontact}}\,. \qquad \text{(A20)}$$

For each timestep, these 20 equations were solved and integrated using Mathematica 5.0 with a RK4 integrator, and a timestep of 5 μs.

LIST OF ABBREVIATIONS

a	anterior
b	body
c	coxa
f	femur
G	ground reaction force
I	inertia
l	lateral
$Length_{\mathrm{f}}$, $Length_{\mathrm{ti}}$, $Length_{\mathrm{m}}$, $Length_{\mathrm{c}}$	lengths of the femur, tibia, moment arm of the trochanteral depressor muscle, coxa
L	left
m	trochanteral moment arm
M	mass
N	normal reaction force at the coxo-trochanteral joint
R	right
ti	tibia
tr	trochanter
$\ddot{x}$, $\ddot{y}$	horizontal and vertical components of acceleration
X,Y	position of the centre of mass on the x- and y-axes
$X_{\mathrm{R\ contact}}$, $Y_{\mathrm{R\ contact}}$	the contact point of the right tibia with the ground
θ_{c}	angle of the coxa with respect to the horizontal
θ_{f} and θ_{ti}	angles between the femur or tibia and the midline
θ_{tr}	angle between the trochanter and the femur
τ	torque

ACKNOWLEDGEMENTS

G.P.S. was supported by the Marshall Sherfield Commission and the Human Frontiers Science Program (HFSP). We would like to thank Jo Riley for her help during the course of this work and our Cambridge colleagues for many helpful discussions and their constructive comments on this manuscript.

REFERENCES

Bennet-Clark, H. C. (1975). The energetics of the jump of the locust *Schistocerca gregaria*. *J. Exp. Biol.* **63**, 53-83.
Bennet-Clark, H. C. and Lucey, E. C. A. (1967). The jump of the flea: a study of the energetics and a model of the mechanism. *J. Exp. Biol.* **47**, 59-76.
Brackenbury, J. (1996). Targetting and visuomotor space in the leaf-hopper *Empoasca vitis* (Gothe) (Hemiptera: Cicadellidae). *J. Exp. Biol.* **199**, 731-740.
Brackenbury, J. and Wang, R. (1995). Ballistics and visual targeting in flea-beetles (Alticinae). *J. Exp. Biol.* **198**, 1931-1942.
Bräunig, P. and Burrows, M. (2008). Neurons controlling jumping in froghopper insects. *J. Comp. Neurol.* **507**, 1065-1075.
Brown, R. H. J. (1967). The mechanism of locust jumping. *Nature* **214**, 939.
Burrows, M. (1969). The mechanics and neural control of the prey capture strike of the Mantid shrimps *Squilla* and *Hemisquilla*. *Z. vergl. Physiol.* **62**, 361-381.
Burrows, M. (1995). Motor patterns during kicking movements in the locust. *J. Comp. Physiol. A.* **176**, 289-305.
Burrows, M. (2003). Froghopper insects leap to new heights. *Nature* **424**, 509.
Burrows, M. (2006a). Jumping performance of froghopper insects. *J. Exp. Biol.* **209**, 4607-4621.
Burrows, M. (2006b). Morphology and action of the hind leg joints controlling jumping in froghopper insects. *J. Exp. Biol.* **209**, 4622-4637.
Burrows, M. (2007a). Anatomy of hind legs and actions of their muscles during jumping in leafhopper insects. *J. Exp. Biol.* **210**, 3590-3600.
Burrows, M. (2007b). Kinematics of jumping in leafhopper insects (Hemiptera, Auchenorrhyncha, Cicadellidae). *J. Exp. Biol.* **210**, 3579-3589.
Burrows, M. (2007c). Neural control and co-ordination of jumping in froghopper insects. *J. Neurophysiol.* **97**, 320-330.
Burrows, M. (2008). Jumping in a wingless stick insect, *Timema chumash* (Phasmatodea, Timematodea,Timematidae). *J. Exp. Biol.* **211**, 1021-1028.
Burrows, M. and Morris, O. (2003). Jumping and kicking in bush crickets. *J. Exp. Biol.* **206**, 1035-1049.
Burrows, M. and Sutton, G. P. (2008). The effect of leg length on jumping performance of short and long-legged leafhopper insects. *J. Exp. Biol.* **211**, 1317-1325.
Burrows, M., Hartung, V. and Hoch, H. (2007). Jumping behaviour in a Gondwanan relict insect (Hemiptera: Coleorrhyncha: Peloridiidae). *J. Exp. Biol.* **210**, 3311-3318.

Burrows, M., Shaw, S. R. and Sutton, G. P. (2008). Resilin and cuticle form a composite structure for energy storage in jumping by froghopper insects. *BMC Biol.* **6**, 41.
Card, G. and Dickinson, M. (2008). Performance trade-offs in the flight initiation of *Drosophila*. *J. Exp. Biol.* **211**, 341-353.
Chiel, H. J. and Beer, R. D. (1997). The brain has a body: adaptive behavior emerges from interactions of nervous system, body and environment. *TINS* **20**, 553-557.
Dickinson, M. H., Farley, C. T., Full, R. J., Koehl, M. A. R., Kram, R. and Lehman, S. (2000). How animals move: an integrative view. *Science* **288**, 100-106.
Eriksson, E. S. (1980). Movement parallax and distance perception in the grasshopper (*Phaulacridium vattatum* (Sjostedt)). *J. Exp. Biol.* **86**, 337-340.
Gray, P. T. A. and Mill, P. J. (1983). The mechanics of the predatory strike of the mantid *Heirodula membranacea*. *J. Exp. Biol.* **107**, 245-275.
Heitler, W. J. (1974). The locust jump. Specialisations of the metathoracic femoral-tibial joint. *J. Comp. Physiol.* **89**, 93-104.
Heitler, W. J. and Burrows, M. (1977). The locust jump. I. The motor programme. *J. Exp. Biol.* **66**, 203-219.
Mallett, E. S., Yamaguchi, G. T., Birch, J. M. and Nishikawa, K. C. (2001). Feeding motor patterns in anurans: Insights from biomechanical modeling. *Am. Zool.* **41**, 1364-1374.
Patek, S. N. and Caldwell, R. L. (2005). Extreme impact and cavitation forces of a biological hammer: strike forces of the peacock mantis shrimp *Odontodactylus scyllarus*. *J. Exp. Biol.* **208**, 3655-3664.
Santer, R. D., Yamawaki, Y., Rind, C. F. and Simmons, P. J. (2005). Motor activity and trajectory control during excape jumping in the locust *Locusta migratoria*. *J. Comp. Physiol. A* **191**, 965-975.
Smith, T. L., Povel, D. G. E. and Kardong, K. V. (2002). Predatory strike of the tentacled snake (*Erpeton tantaculatum*). *J. Zool. Lond.* **256**, 233-242.
Sobel, E. C. (1990). The locust's use of motion parallax to measure distance. *J. Comp. Physiol. A* **167**, 579-588.
Sutton, G. P. and Burrows, M. (2008). The mechanics of elevation control in locust jumping. *J. Comp. Physiol. A* **194**, 557-563.
Van Leeuwen, J. L. and Kier, W. M. (1997). Functional design of tentacles in squid: Linking sarcomere ultrastructure to gross morphological dynamics. *Philos. Trans. R Soc. Lond., B, Biol. Sci.* **352**, 551-571.
Van Wassenbergh, S. and Aerts, P. (2009). Aquatic suction feeding dynamics: insights from computational modelling. *J. R. Soc. Interface* **6**, 149-158.
Wainwright, P., Carroll, A. M., Collar, D. C., Day, S. W., Higham, T. E. and Holzman, R. A. (2007). Suction feeding mechanics, performance, and diversity in fishes. *Integr. Comp. Biol.* **47**, 96-106.